Chemical Engineering Journal 96 (2003) 117–124

Chemical Engineering Journal

www.elsevier.com/locate/cej

Structuring chaotic fluidized beds

Marc-Olivier Coppens*, J.R. van Ommen

Department of Chemical Technology, Faculty of Applied Sciences, Delft University of Technology, Julianalaan 136, 2628 BL Delft, The Netherlands

Abstract

Three new ways are proposed to "structure" bubbling gas–solid fluidized beds, i.e. to bring order into their chaotic hydrodynamics. Just like for fixed bed reactors, the rational structuring of fluidized beds, a novel concept, is interesting from the point of view of process intensification, to facilitate scale-up and control, and to improve performance. Applying an AC electric field, reduces the average bubble size by manipulating interparticle forces. Introducing part of the gas via a fractal injector, immersed into the bed, homogenizes the bed contents, considerably improves gas–solid contact, and simplifies scale-up. Oscillating the gas flow transforms chaotic bubble motion into remarkably regularly ordered patterns of rising bubbles.

Keywords: Fluidized bed; Structured reactors; Chaos; Fractal; Electric fields; Self-assembly; Chaos-order transition

1. Introduction

Pioneering research by van den Bleek at Delft has been instrumental in building a different and particularly useful perspective on gas–solid fluidization. Fluidization is the basis for scores of applications in which fast heat and mass transfer between gas and solids as well as fast cooling or heating the gas–solid mixture is essential. Therefore, improved understanding and accurate modeling are important, yet gas–solid fluidization remains a notoriously difficult to quantify phenomenon. Consider a bubbling fluidized bed. In such a system, gas is typically distributed via a bottom distributor plate into a vessel filled with solid particles with which the gas interacts: the gas could dry the particles, contain reagents to coat them, react with them or be involved in reactions catalyzed by the particles. Above a certain velocity, the solid particles are fluidized. The gas–solid suspension becomes unstable at this same velocity (the so-called minimum fluidization velocity, U_{mf}), or at a slightly higher velocity, so that bubbles appear (past the minimum bubbling velocity). These bubbles grow while rising through the vessel, possibly coalescing and perhaps breaking up again. Their motion is irregular. Also the solids circulate in complex scale-dependent patterns. Therefore, the hydrodynamics of bubbles and of the surrounding suspension or emulsion phase in such a gas–solid fluidized bed are very complex. Interestingly, however, the dynamics are not just complicated: van den Bleek and Schouten [1] and Daw et al. [2] have shown that fluidized beds can be regarded as chaotic systems, in the mathematical sense of the word. The chaos approach towards fluidized beds allows replacing purely empirical descriptions by models that account for a more fundamental quantitative characterization of the dynamic behavior such as the chaotic attractor of the system or the Kolmogorov entropy, and their dependence on the gas–solid properties. A recent review paper [3] summarizes the results based on this chaos theoretical approach, varying from scaling up fluidized beds to monitoring hydrodynamic changes and controlling fluid bed dynamics, hereby controlling fluidized bed processes. In other words, the discovery that a fluidized bed is chaotic is of more than scientific interest, and is more useful in engineering applications.

Also computational fluid dynamics simulations on faster and faster computers provide new insight into fluidization. Such improved understanding and models of fluidization may help to take a next step, which is of fundamentally different reactor design and operation, based on *rational* as opposed to *empirical* methods. Many ways to improve the fluidization behavior for particular applications have already been proposed and several are applied on an industrial scale, but most of these are empirical or do insufficiently rely on fundamental insights. Examples are the use of baffles, changes in gas distributor design, application of magnetic or electric fields, the use of sound waves, pulsating the gas flow, and vibrating the bed or the distributor. Most of this work is purely empirical in nature. By changing the fluidization behavior in a more rational way, based at least

* Corresponding author. Tel.: +31-15-278-4399; fax: +31-15-278-8668.
E-mail address: m.o.coppens@tnw.tudelft.nl (M.-O. Coppens).

1385-8947/$ – see front matter © 2003 Elsevier B.V. All rights reserved.
doi:10.1016/j.cej.2003.08.007

Nomenclature

D	fractal dimension of a tree
D_B	bubble size (m)
f	oscillation frequency (Hz)
m	number of segments
n	fractal generation number
Q_a	oscillation amplitude (m^3/s)
Q_{mf}	minimum fluidization flow rate (m^3/s)
Q_p	primary flow rate (m^3/s)
Q_s	secondary flow rate (m^3/s)
t	time (s)
U_{mf}	minimum fluidization velocity (m/s)
U_p	primary gas velocity (m/s)

Greek letters

δ	inner cutoff (m)
Δ	diameter exponent of a tree

partially on new fundamental insights, the hydrodynamics could be changed in a significant and controlled way, so as to have a better control over the system, and improve mass and heat transfer.

The aim of our most recent research at Delft, inspired by the work of van den Bleek, is ab initio control via a rational design and operation of fluidized beds. This is reminiscent of ongoing work in our department in fixed bed reactor design: ab initio control and higher efficiencies can be achieved by replacing random catalyst packings by structured packings, such as monoliths or regular packings of individual catalyst particles [4,5]. We will show how, in fluidization technology, novel reactor designs, gas distributor designs and controlling the gas inlet dynamics may similarly enable us to "*structure*" fluidized beds. Three examples are discussed: manipulation of interparticle forces via AC electric fields, fractal injection of gas into the system, and pulsation of the gas flow.

2. AC electric fields: bubble size reduction

The application of an alternating AC electric field is one of the methods we investigate for controlling the bubble size in a fluidized bed. We will give a short overview here. This work is more extensively described by Kleijn van Willigen et al. [6,7]. In fluidized beds, the forces on the particle scale are extremely important for the hydrodynamic behavior on the meso-scale. By applying an AC electric field to a fluidized bed of semi-insulating particles, we obtain additional possibilities to control the interparticle forces and thus the hydrodynamic behavior. By definition, a state of fluidization exists when the force of gravity on the particles is balanced by the drag arising from the flow of the fluidizing gas. Consequently, small interparticle forces (e.g. Van der Waals forces), which may not be noticeable in other circumstances,

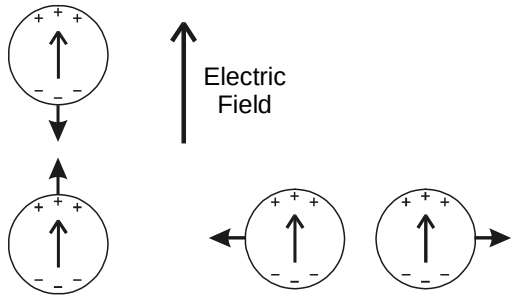

Fig. 1. Electric forces between particles polarized in an electric field (adapted from [11]).

may have observable consequences when the particles are fluidized [8–10].

In the presence of an electric field, semi-insulating particles (e.g. glass beads) become polarized, leading to an attractive or repulsive interparticle force, depending on their relative orientation in the electric field (Fig. 1). The maximum strength of this interparticle force is comparable in magnitude to the drag and gravity forces exerted on fluidized glass beads with a diameter of about 80 μm. For larger particles, the polarization forces become (much) smaller than drag and gravity, but can still play a significant role. For an AC electric field, the particles will periodically experience a cohesive force in the direction of the field. For the right values of field strength and frequency, the cohesive force in the field direction can lead to the temporary formation of loose particle strings. These strings may hinder the formation, movement, and/or coalescence of the bubbles.

In the earliest work on electric fields in fluidized beds, researchers focused mainly on what was called the "stabilization" of a fluidized bed: constant (DC) electric fields were applied that completely "froze" the fluidized bed, e.g. [12,13]. Later on, the focus shifted more towards AC electric fields. Here, the forces between the particles vary in time, maintaining fluidization of the bed, e.g. [14,15]. Nevertheless, the effect on the bed was mainly evaluated by bed expansion and visual observations. Currently, we are applying more advanced measurement and analysis techniques (video image analysis and pressure fluctuation analysis) to obtain detailed information about the bubble characteristics. This additional information will make it easier to optimize the electrical field configuration and will eventually lead to a more complete picture of the relation between micro-scale polarization forces and the meso-scale changes in the bubble characteristics.

2.1. Freely bubbling experiments

The effect of an electric field on a fluidized bed will be illustrated by experiments carried out in a pseudo-two-dimensional (2D) fluidized bed set-up with an internal cross section of 20 cm × 1.5 cm. The electrodes consist of a regular wire pattern strung through the column front and rear, passing through the bed. The porous sintered steel sieve plate

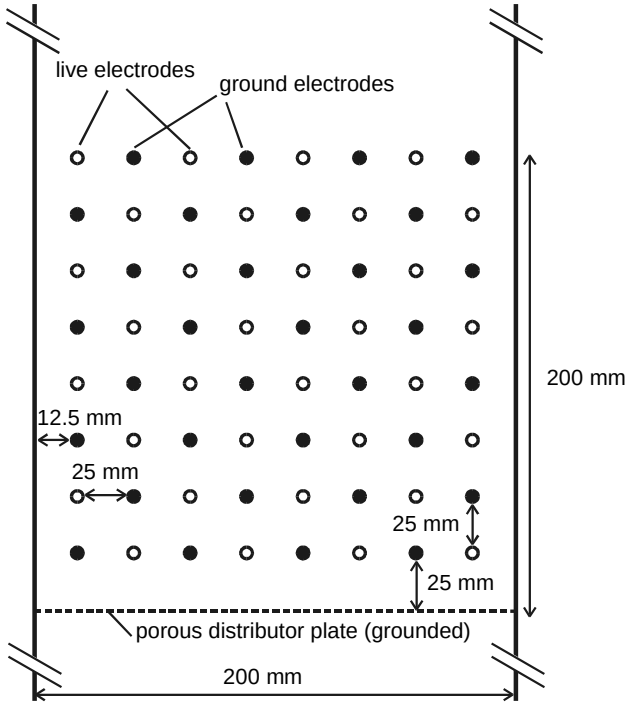

Fig. 2. Side view of the electrode configuration in the pseudo-2D column. Open circles represent live electrodes, while filled circles represent grounded electrodes.

is grounded, and therefore serves as one of the electrodes. The NiCr wire electrodes (diameter 250 μm) are alternately, both horizontally and vertically, grounded or connected to a Trek 20/20c high-voltage power amplifier (Fig. 2). The electrodes thus create a quadruple field with horizontal and vertical components. A more detailed description of the set-up can be found in Kleijn van Willigen et al. [6].

At a height of 1, 10, 19, and 30 cm above the support plate, pressure fluctuations were measured at the wall using Kistler piezo-electric pressure transducers, type 7261. These pressure transducers measure the pressure fluctuation relative to the average pressure. The pressure fluctuation time-series measured at different heights in the column were analyzed to determine changes in the average bubble size with changing electric properties. Van der Schaaf et al. [16] proposed a way to decompose the power spectral density of pressure fluctuations into a part generated by global phenomena and a part generated by bubble passage. From the latter part, a characteristic length scale of the bubbles can be calculated. This method was used in the present experiments to determine the effect of an electric field for a range of frequencies and field strengths. The change in bubble size was always determined relative to the bubble sizes without an electric field.

We will show the results for freely bubbling bed experiments for two types of particles. The bubble size reduction as a function of field strength and frequency is given in Fig. 3, which shows the effect of the electric fields on 77 μm glass beads (Geldart A particles), fluidized with dry air at a superficial velocity of 0.03 m/s ($\sim 3U_{mf}$). The settled bed height was 0.30 m. It was visually observed that the particles kept moving, and under no condition the bed was frozen. Bed expansion during fluidization with and without electric fields was visually observed to be very similar, but the pressure fluctuation analysis shows that the bubble diameter changes significantly. The measured reduction in bubble diameter at the measuring height shown is about 25%, which corresponds to a decrease in bubble volume (assuming spherical bubbles) of approximately 60%. A comparable reduction in bubble size has been obtained in a fully three-dimensional (3D) fluidized bed [6]. Fig. 3a shows that for frequencies from 5 to 20 Hz, the effect of the electric field is largest. This is in reasonably good agreement with particle time constants given by Colver [15].

Fig. 3b shows the results for similar experiments with larger glass beads (700 μm diameter, Geldart B) fluidized

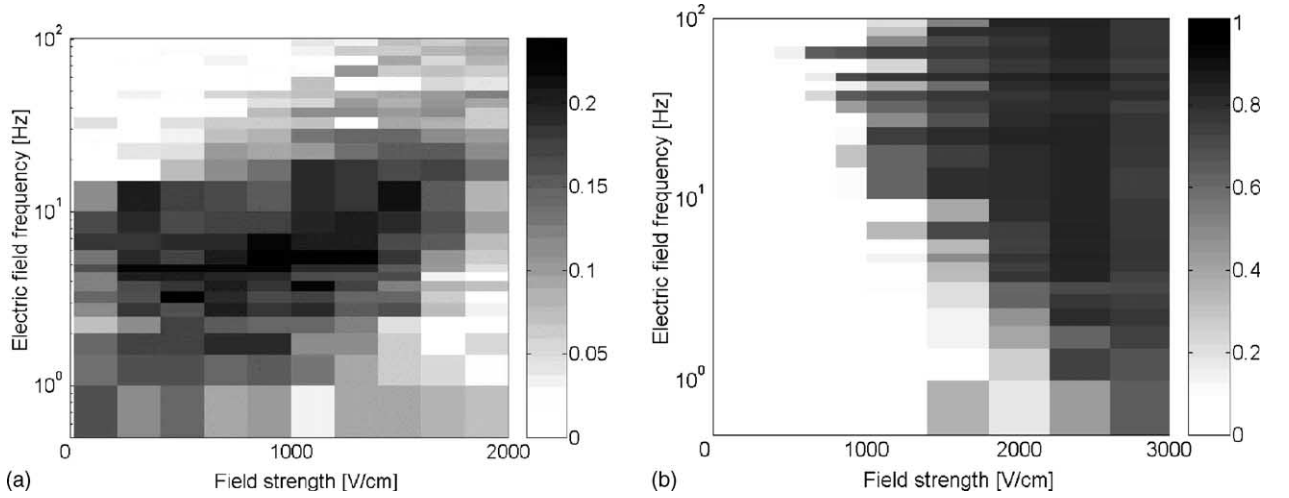

Fig. 3. Bubble size reduction calculated from pressure fluctuations measured at 190 mm above the distributor plate as a function of frequency and applied field. The grayscale displays the reduction as a fraction of the mean bubble diameter for the situation without imposing a field. Bed material: (a) 77 μm glass beads; (b) 700 μm glass beads.

at 0.50 m/s ($\sim 1.5U_{mf}$). The results show a much larger decrease in mean bubble diameters than for the smaller particles—a drop of up to 85% as compared to the situation without electric fields. A dependence on frequency and voltage is again evident. It seems this region extends beyond the ranges used in these experiments. The effect of the electric fields is most pronounced at somewhat higher frequencies than for the smaller Geldart A particles. We do not have an explanation yet for this counterintuitive result. In contrast to the Geldart A experiments, there is clearly a minimum field strength required for the Geldart B particles to experience changes in bubble size. This is reasonable, since the drag and gravity force are a factor 1000 larger than for the Geldart A particles.

2.2. Bubble injection experiments

More detailed information about bubble size, bubble shape, and the number of bubbles is obtained from video analysis of bubble injection experiments. The column with its electrode wiring is the same as above, except that a 10 cm extension piece was placed between support plate and the first electrodes to allow the formation of bubbles without the influence of the electric fields. A bed of 520 μm glass bead particles was fluidized with dry air at 0.28 m/s, just above the minimum fluidization velocity (0.24 m/s). The settled bed height was 0.44 m. Two weight percent of fines were added to the bed material to smoothen fluidization. A gas pulse of 90 cm^3 was injected through the center of the bottom plate into the bed, forming one or more bubbles. The experiments are repeated about 60 times to obtain reliable statistics. Images were captured on a digital video camera at a frame rate of 25 frames/s. The system was illuminated from behind.

The video analysis showed that the bubbles injected at the bottom plate are broken up when they move into the electrode region. Fig. 4 gives the probability density functions for the bubble diameter and the number of bubbles per video frame as obtained from the image analysis. The data are shown for the top 5 cm of the electrode region for a no-field situation, a 2 Hz, and a 10 Hz field of 5 kV/cm. Fig. 4a shows a large decrease in bubble diameter under the influence of the electric fields in the electrode region, which is in agreement with the results for the freely bubbling bed. Fig. 4b shows that the average number of bubbles per video frame increases by imposing an electric field. However, the increase in bubble number does not compensate for the decrease in bubble size: the total visual bubble volume decreases strongly (~50%) under the presence of an electric field. This suggests that part of the gas is moved to the emulsion phase. Both bubble size reduction and an increased amount of emulsion phase gas will increase the gas-to-solid mass transfer.

3. Fractal injector: suppressing bubbles

Gas is traditionally introduced via a bottom distributor plate. However, as long as the reactor contents remain fluidized, part of the gas could be introduced at different locations in the bed, and not only from below. Such secondary gas injection lends additional flexibility to fluidized bed operation, and these additional degrees of freedom can obviously be used to improve the reactor performance. When, on top of this, the device used to inject the gas is given a fractal design (Fig. 5), scale-up of the controlled hydrodynamics is facilitated [17–19].

The amount of gas introduced via the bottom distributor plate is called the "primary" flow (Q_p), while the gas introduced via a fluid injector to different locations inside the bed is called the "secondary" flow (Q_s). By maintaining the primary gas flow Q_p above Q_{mf} ($U_p \geq U_{mf}$), the gas–solid mixture remains fluidized. If the total gas flow rate Q_0 to be introduced in the bed is much larger than the minimum fluidization velocity (for simplicity, here we only consider Geldart B powders, with $Q_b = Q_{mf}$), large bubbles would be formed if all the gas were to be introduced as primary gas. For processes limited by the transport of active components between gas and solid particles, this is disadvantageous. By spreading out part of the gas, Q_s, over several

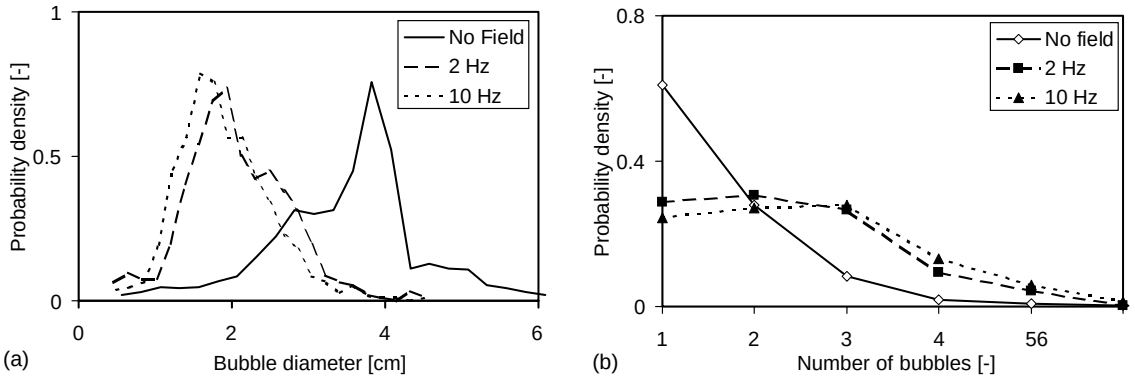

Fig. 4. (a) Diameter of the bubbles and (b) number of bubbles in the top 5 cm of the electrode region as obtained from video recordings of the bubble injection experiments.

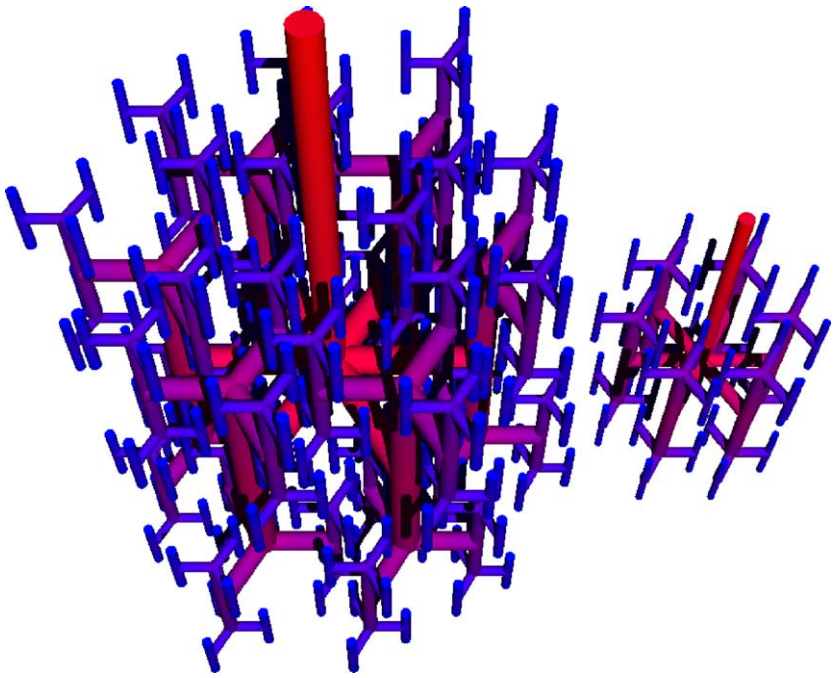

Fig. 5. Example of self-similar fractal injectors with a fractal dimension $D = \log 6/\log 2 \approx 2.58$. The left one could be used in a large reactor vessel, scaled up from the smaller vessel in which the right one would be used. These tree-like injectors only differ in their number of branching levels or generations, n. Fluid enters the stem, and exits the multitude of smallest twigs. Equal path lengths from stem to twigs help to uniformize the exiting fluid, whatever the size of the vessel.

locations higher up in the bed, while the primary flow Q_p is only slightly above Q_{mf}, a number of desirable features may be attained.

First, fresh gas is fed to regions where rising gas is (partially) depleted from active components. Multiple gas injection points along the vertical direction will lead to behavior closer to plug flow, and a virtual division of the fluidized bed into different well-mixed regions or cells, which are in direct contact with each other.

Second, incoming fresh gas, flowing into the reactor through the injector outlets, mixes with the already present gas–solid suspension, leading to enhanced local mixing within the virtual cells. By injecting gas at different locations at the same bed height, possible radial inhomogeneities are diminished or eliminated as well.

Third, bubble formation may be suppressed, as illustrated in Fig. 6. Bubbles only gradually grow while gas rises through a fluidized bed. A fluidized bed is a dynamic system, and it takes time for an unstable gas–solid mixture to separate into gas bubbles and a gas–solid suspension with a void fraction close to that at minimum fluidization, i.e. the thermodynamic equilibrium. Therefore, in a conventional, deep bubbling fluidized beds with only primary flow, this (thermo)dynamic equilibrium is only reached higher up in the bed. When secondary gas is injected at different heights, before the equilibrium is reached, a suspension with a gas fraction higher than the equilibrium fraction may be dynamically sustained. Freshly injected gas at different vertical locations disperses particles and breaks up bubbles, so that a metastable suspension with high gas content is formed. The improved gas–solid contact as a result of the just discussed process, amply compensates for the small reduction in average residence time, for transport-limited processes.

Secondary gas injection can be taken optimally advantage of by introducing the gas at optimized locations throughout the bed. These locations will depend on the process at hand, but giving the injector itself a fractal shape facilitates scale-up and homogenization. Tree-like fractal injectors, such as the ones shown in Figs. 5 and 6, allow to inject the gas flow via a single stem, and subdivide it in equal parts by repeated branching, in such a way that the distance from the stem to each of the outlets is equal. Equal pressure drops and equal exit flows may hence be realized. Furthermore, fractals are intrinsically scalable, as exemplified by (real) natural trees. A fractal design makes it easier to maintain the uniformity even while scaling up a reactor, hereby avoiding scale-dependent hydrodynamics. An additional bonus is that the injector tubes themselves may function as a static mixer. This was noticed when operating a scaled-up version of the injector shown in Fig. 6, twice as high and twice as wide, with 64 outlets (instead of 16) in a 40 cm bed (instead of a 20 cm one), at $U = 6U_{mf}$: even without injecting gas through the injector, its presence alone already reduced bubble size. The bubble size was further reduced when part of the gas was led through the injector.

Fractal trees are characterized by several parameters, like their fractal dimension, D, their diameter exponent, Δ, and the number of branching levels, n [20]. Both the length and

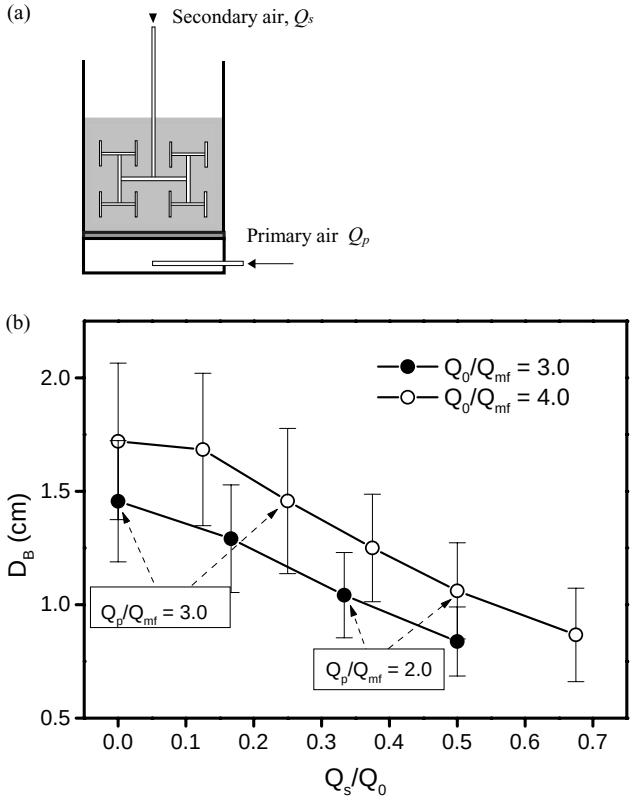

Fig. 6. Illustration of the decrease in average bubble size, D_B, calculated from the analysis of video images of air-fluidized 2D beds of 200 μm sand particles, when a fractal gas injector, as shown in (a), is used. A part Q_s of the total flow Q_0 is distributed via a 2D fractal injector, while the rest, Q_p, is injected through the porous bottom plate. In these experiments, the (pseudo) 2D bed was 20 cm wide, 20 cm deep, and 1.5 cm thick.

the diameter of the injector tubes decrease as power laws, characterized by D and Δ, respectively. It is clear that thicker tubes take more space, but that they also reduce the pressure drop over the device, so there will be an optimum for Δ. The optimization of the fractal dimension D is an independent matter, yet a non-trivial one. We can only briefly touch upon the subject here, but it can be shown easily that D will in general be less than 3 and more than 2. On the one hand, the injected fluid ought to reach the complete reactor volume, but on the other hand, it is not desirable to have a space-filling device ($D = 3$ for a 3D bed or $D = 2$ for a pseudo-2D one), which is complicated, occupies much space, and more, importantly, performs sub-optimally. The latter is a result of the dynamic behavior of the system and the intrinsic anisotropy. If the reactor contents were static, a uniform and as dense as possible distribution of secondary injection points would lead to uniform reaction conditions. However, both primary and secondary gas rise through the bed, which means that, in general, it is better to distribute the injection points in a non-uniform way in the axial direction. The distribution depends on the kinetics of the fluidized bed process, and the mass transfer limitations (which we try to eliminate). Furthermore, out flowing secondary gas mixes with the local contents in the reactor. The distance between outlets, horizontally and vertically, can be optimized based on the local mixing properties. Note that this optimization could be performed based on single outlet studies, as a result of the fractal scaling properties of the injector, and the localization of the mixing. Local mixing can and should be taken advantage of: a higher density of outlets is not better. The outlet design could be independently optimized to improve local mixing. Finally, it is interesting to think about fractal "trees" in nature, like botanical trees, lungs, kidneys, or the vascular network, which are all fractal yet have different geometries depending on their function. Also in nature, the chosen and perhaps also optimal parameters (in particular, D and Δ) take on different values depending on the function of the tree.

An often forgotten concept from fractal geometry, introduced by Mandelbrot [20], is lacunarity. The lacunarity describes how close (low lacunarity) or how far (high lacunarity) a fractal is removed from homogeneity. As discussed by Coppens [21], lacunarity should play a crucial role in optimizing the structure of the fractal injector as the fractal dimension alone is clearly insufficient to characterize even the simplest fractal (Fig. 7). In particular, by tuning the lacunarity it is possible to realize homogeneity, even at fractal dimensions D inferior to those of the embedding space, i.e. $D < 3$ for a 3D fluidized bed. In other words, the lengths of the tubes and the number of outlets scale with reactor size as a power law with $D < 3$, to maintain the desired properties in each outlet "cell", yet the distance between these outlets is controlled independently to maintain a desired uniform or non-uniform distribution—the non-uniformity to compensate for reactor anisotropy. Future work will explore the optimization of the fractal injector, and its use in chemical processes, in more detail.

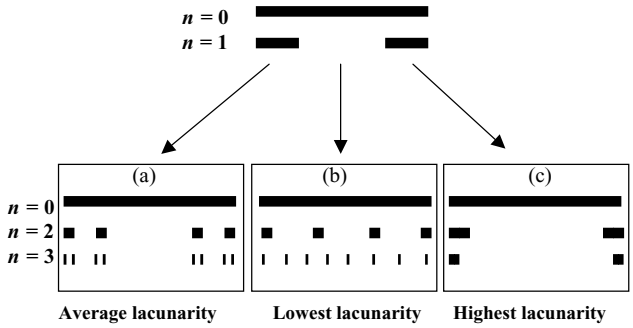

Fig. 7. Fractal lacunarity measures deviations from translational homogeneity. All shown (pre-)fractal (Cantor) sets share the same Hausdorff (fractal) dimension: $D = \log 2/\log 4 = 1/2$, since the number of segments, m, scales with the fractal generation, n, as $m \sim 2^n$, while the size of the inner cutoff, δ, scales as $\delta \sim 4^{-n}$, and $D = -\log m/\log \delta$. Nevertheless, the distribution of the voids, a measure for lacunarity, differs in each case. In (a) the voids are distributed in a non-uniform way and have a size distribution that is a power law characterized by D (the conventional, self-similar Cantor set). The voids in (b) are distributed uniformly and have a size $\delta \sim 4^{-n}$ each. The voids in (c), finally, all shrunk to zero except for one void of size $1–2^{-n}$ that in the limit covers the entire length (extreme non-uniformity).

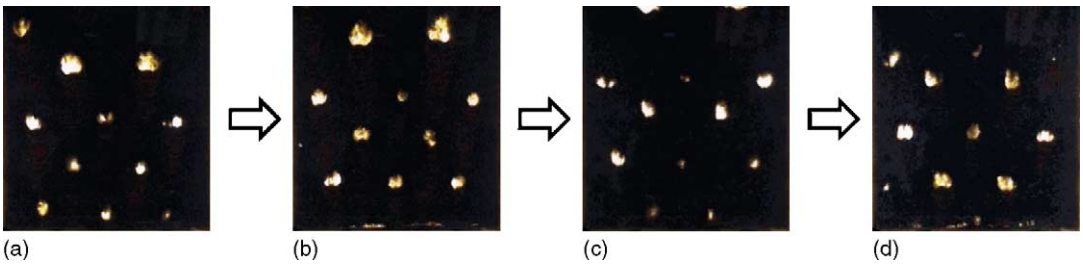

Fig. 8. Dynamic, ordered bubble patterns form in a deep, yet thin ("2D") air-fluidized bed of sand particles (43 cm high × 40 cm wide), when the airflow is oscillated at a frequency $f = 3.5$ Hz, and $Q_p = Q_{mf}$; $Q_a = 0.5Q_{mf}$. The sequence shows four snapshots out of one period of the bubble pattern (frequency $3.5/2 = 1.75$ Hz), as seen through the front of the bed [26].

4. Pulsating fluidized beds: ordering the chaos

A third way to modify the fluidized bed hydrodynamics in a considerable way, without changing the average gas flow, is to oscillate the gas flow around the average instead of keeping it constant. Work by Massimilla et al. [22] had indicated that oscillating the gas flow could notably improve the efficiency of fluidized bed combustion. Wong and Baird [23] and Köksal and Vural [24] showed that periodic pulsation of the gas flow would influence the bubble size and could be used to improve fluidized bed performance. Furthermore, it is known that chaotic dynamics can be locked into a periodic orbit by fluctuating certain parameters that influence the dynamics—chaos control [3], and Pence and Beasley [25] showed that pulsed fluidization could indeed suppress chaotic behavior.

All this inspired us to oscillate the gas flow in a (pseudo) 2D fluidized bed, one with similar characteristics as the one used in experiments with the fractal injector. This time, all gas was injected through the porous distributor plate, but a sinusoidally oscillating gas flow, $Q_a[1 + \sin(2\pi ft)]$, was superimposed onto a constant primary gas flow, $Q_p > Q_{mf}$, so that the total gas flow $Q_0 = Q_p + Q_a[1 + \sin(2\pi ft)]$ would always be above minimum fluidization. For a broad range of frequencies f (on the order of a few Hertz: 2.5–7 Hz) and amplitudes ($Q_a/Q_{mf} = 0.2$–0.7), very regular bubble patterns would appear. Bubbles would rise in staggered, regularly ordered rows (Fig. 8) [26]. Knowing that "bubbles" are actually dynamic voids [27], which are far from being perfectly smooth entities, this is even more remarkable. At a certain bed height, the order is destroyed, and the bubble patterns again turn chaotic. Interestingly, the pattern formation and the inter-bubble distance in the pattern are independent of bed width, as long as gas is introduced in a uniform way through the porous bottom distributor plate. Uniformly injected gas very quickly rearranges itself to form a regular row of bubbles, which rises vertically through the bed. Near the maximum of every oscillation period, a new row of bubbles is formed, staggered with respect to the previous row. Instabilities, partially intrinsic, partially caused by the walls, ultimately lead to disappearance of the order higher up in the bed. Since wall effects are smaller when the bed is wider, the patterns survive up to a height that seems to be almost equal to the width, at least in the experiments with air and sand performed up to now. The waves are no simple linear resonance phenomenon. The pattern wavelength is not inversely proportional to the driving frequency, while the pattern is formed in a range of frequencies and not at specific frequencies.

Many perturbed, non-linear dissipative systems driven outside of equilibrium are known to generate regular patterns [28]. Fluctuations may lead to self-assembly and pattern formation [29]. At the same time, patterns are a signature of the system properties, so the formation of patterns in fluidized beds may not only be a way to order them, but at least as relevant is that patterns and their characteristics reveal something about the underlying complex dynamics.

In cylindrical columns, filled with a shallow layer of sand and fluidized by an oscillating airflow, regular patterns were also discovered [27], very similar to the ones seen in vibrated granular layers [29,30]. Ordered patterns in 2D or 3D vibrated granular layers, however, are only formed when the layers are very shallow, as a result of extensive dissipation via interparticle collisions, while the experiments in the (deep, vertical) pseudo-2D bed showed that patterns are propagated by the gas flow up to considerable macroscopic heights.

5. Conclusions

This paper introduced three possibilities to structure chaotic fluidized beds, the aim of which is to increase control over fluidized bed hydrodynamics by fundamental changes in reactor operation and gas distributor design.

The AC electric fields give us the possibility to directly manipulate the interparticle forces due to polarization effects. In this way, a considerable reduction in bubble size can be achieved while maintaining fluidization, thus enhancing the gas–solid contact, which is beneficial in transport-limited fluidized bed processes.

Using secondary gas injection, bubble formation can also be suppressed, and gas–solid suspensions with a high porosity can be maintained. Giving the secondary gas injector a

fractal design, facilitates scale-up of fluidized beds, as a result of the intrinsic scaling property of fractals.

Oscillating the gas flow that is introduced at the bottom of the fluidized bed may lead to the transformation of chaotic to stable, remarkably regular bubble patterns, offering new avenues for intrinsic control and scale-independent hydrodynamics.

Research on "structured" fluidized beds is at an early stage. Concrete technological applications will be evaluated in future work. On the fundamental scientific side, future research on structured fluidized beds will increasingly rely on the manipulation of interparticle forces and particle–fluid interactions to achieve a desirable fluidization behavior for a given application. The combination of microscopic and mesoscopic modeling with careful experimentation is essential in obtaining more insight in fluidization and in controlling the chaos.

Acknowledgements

Current and former group members are thanked for their contributions to this research, in particular: F. Kleijn van Willigen, G.B. Schmit, S. Baltussen, Y. Cheng, S. Lems, and M.A. Regelink. Professor J. van Turnhout is thanked for fruitful discussions concerning the electric fields. The authors would like to thank Professor Cor M. van den Bleek for the many stimulating and inspiring discussions. One of the authors (M.-O.C.) would like to thank the Dutch Foundation for Scientific Research, NWO, for ongoing financial support via an Open Competition grant, and a Jonge Chemici (Young Chemist) and a PIONIER award.

References

[1] C.M. van den Bleek, J.C. Schouten, Deterministic chaos—a new tool in fluidized-bed design and operation, Chem. Eng. J. 53 (1993) 75–87.
[2] C.S. Daw, W.F. Lawkins, D.J. Downing, N.E. Clapp, Chaotic characteristics of a complex gas–solids flow, Phys. Rev. A 41 (1990) 1179–1181.
[3] C.M. van den Bleek, M.-O. Coppens, J.C. Schouten, Application of chaos analysis to multiphase reactors, Chem. Eng. Sci. 57 (2002) 4763–4778.
[4] H.P.A. Calis, J. Nijenhuis, B.C. Paikert, F.M. Dautzenberg, C.M. van den Bleek, CFD modelling and experimental validation of pressure drop and flow profile in a novel structured catalytic reactor packing, Chem. Eng. Sci. 56 (2001) 1713–1720.
[5] F. Kapteijn, T.A. Nijhuis, J.J. Heiszwolf, J.A. Moulijn, New non-traditional multiphase catalytic reactors based on monolithic structures, Catal Today 66 (2001) 133–144.
[6] F. Kleijn van Willigen, J.R. van Ommen, J. van Turnhout, C.M. van den Bleek, Bubble size reduction in a fluidized bed by electric fields, Int. J. Chem. React. Eng. 1 (2003) (paper A21). http://www.bepress.com/ijcre/vol1/A21.
[7] F. Kleijn van Willigen, J.R. van Ommen, J. van Turnhout, C.M. van den Bleek, The influence of AC electric fields on bubbles in gas–solids fluidized beds, in: Proceedings of the 11th International Conference on Fluidization, submitted for publication.
[8] K. Rietema, The Dynamics of Fine Powders, Elsevier, Dordrecht, 1991.
[9] J.P.K. Seville, C.D. Willett, P.C. Knight, Interparticle forces in fluidisation: a review, Powder Technol. 113 (2000) 261–268.
[10] J.M. Valverde, M.A.S. Quintanilla, A. Castellanos, P. Mills, Experimental study on the dynamics of gas-fluidized beds, Phys. Rev. E 67 (2003) (article no. 016303).
[11] M. Parthasarathy, D.J. Klingenberg, Electrorheology: mechanisms and models, Mater. Sci. Eng. R 17 (1996) 57–103.
[12] T.W. Johnson, J.R. Melcher, Electromechanics of electrofluidized beds, Ind. Eng. Chem. Fundam. 14 (1975) 146–153.
[13] P.W. Dietz, J.R. Melcher, Interparticle electrical forces in packed and fluidized beds, Ind. Eng. Chem. Fundam. 17 (1978) 28–32.
[14] M. Zahn, S.-W. Rhee, Electric field effects on the equilibrium and small signal stabilization of electrofluidized beds, IEEE Trans. Ind. Appl. IA-20 (1) (1984) 137–147.
[15] G.M. Colver, An interparticle force model for AC–DC electric fields in powders, Powder Technol. 112 (2000) 126–136.
[16] J. Van der Schaaf, J.C. Schouten, F. Johnsson, C.M. van den Bleek, Non-intrusive determination of bubble and slug length scales in fluidized beds by decomposition of the power spectral density of pressure time series, Int. J. Multiphase Flow 28 (2002) 865–880.
[17] M.-O. Coppens, Geometrical control of multiphase processes using a new fluid injection system, in: Proceedings of the AIChE Annual Meeting, Dallas, TX, USA, 31 October–5 November, Paper 288c, 1999.
[18] M.-O. Coppens, Method for operating a chemical and/or physical process by means of a hierarchical fluid injection system, US Patent 6,333,019 (2001).
[19] Y. Cheng, C.M. van den Bleek, M.-O. Coppens, Hydrodynamics of gas–solid fluidized beds using a fractal injector, in: M. Kwauk, J. Li, W.-C. Yang (Eds.), Proceedings of the 10th International Conference on Fluidization, United Engineering Foundation, New York, 2001, pp. 373–380.
[20] B.B. Mandelbrot, The Fractal Geometry of Nature, Freeman, San Francisco, CA, 1983.
[21] M.-O. Coppens, Nature inspired chemical engineering—learning from the fractal geometry of nature in sustainable chemical engineering, Proc. Symp. Pure Math., in press.
[22] L. Massimilla, G. Volpicelli, G. Raso, A study on pulsating gas fluidization of beds of particles, Chem. Eng. Prog. Symp. Ser. 62 (1966) 63–70.
[23] H.W. Wong, M.H.I. Baird, Fluidization in a pulsed gas flow, Chem. Eng. J. 2 (1971) 104–113.
[24] M. Köksal, H. Vural, Bubble size control in a two-dimensional fluidized bed using a moving double plate distributor, Powder Technol. 95 (1998) 205–213.
[25] D.V. Pence, D.E. Beasley, Chaos suppression in gas–solid fluidization, Chaos 8 (1998) 514–519.
[26] M.-O. Coppens, M.A. Regelink, C.M. van den Bleek, Pulsation induced transition from chaos to periodically ordered patterns in fluidised beds, in: Proceedings of the Fourth World Conference on Particle Technology, Paper 355, 2002.
[27] J.G. Yates, D.J. Cheesham, Y.A. Sergeev, Experimental observations of voidage distribution around bubbles in a fluidized bed, Chem. Eng. Sci. 49 (1994) 1885–1895.
[28] M.C. Cross, P.C. Hohenberg, Pattern formation outside of equilibrium, Rev. Mod. Phys. 65 (1993) 851–1112.
[29] T. Shinbrot, F.J. Muzzio, Noise to order, Nature 410 (2001) 251–258.
[30] T.H. Metcalf, J.B. Knight, H.M. Jaeger, Standing wave patterns in shallow beds of vibrated granular material, Physica A 236 (1997) 202–210.